CHAPTER 4
RESULTS AND DISCUSSION

4.1 Sequence alignment

From sequence alignment of five MscL homologues shown in Figure 4.1, a general overall similarity for all regions of the protein was observed. However, the two transmembrane regions has greater conservation than the extracellular loop or C-terminal regions. The TM1 domain appears to be the most conserved region whereas the extracellular loop is the most variable region. The sequence identity and sequence similarity of *Mtb*MscL compared with *Eco*MscL is 37% and 73%, respectively.

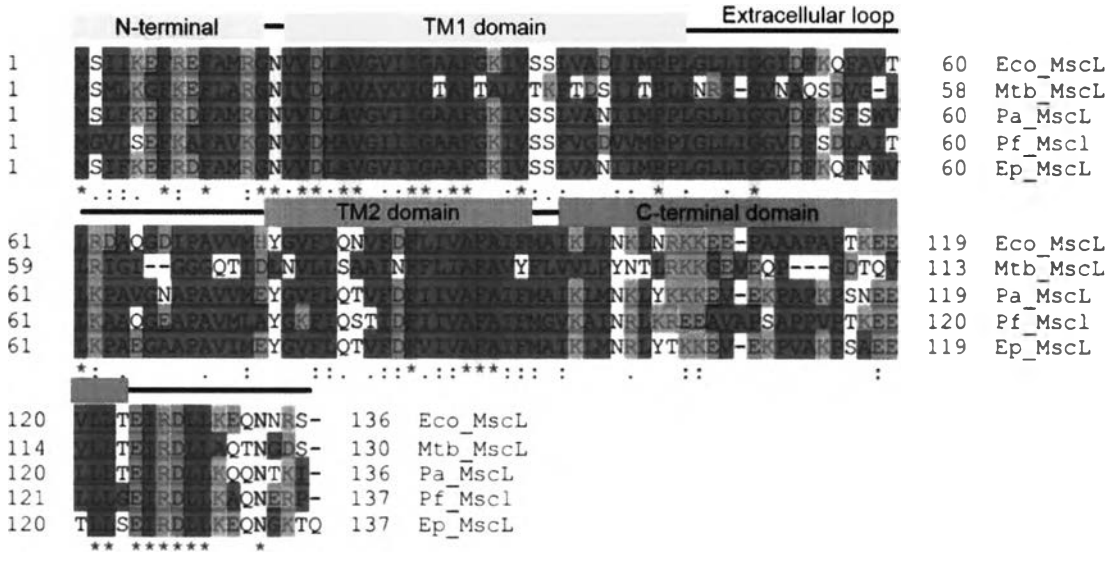

FIGURE 4.1 Primary sequence alignment of MscL channels from various microorganisms: Eco = *Escherichia coli*, Mtb= *Mycobacterium tuberculosis,* Pa= *Pantoea ananatis*, Pf= *Plasmodium falciparum*, Ep= *Erwinia pyrifoliae*.

4.2 PaDSAR models of cl-ecoMscL and in-ecoMscL

Three-dimensional structural models of ecoMscL for closed and intermediate conformations were obtained based on PaDSAR method and the solvent accessibility data. Figure 4.2, illustrates a homopentameric model of the closed and intermediate conformations of ecoMscL. Each monomer of ecoMscL channel consists of 136 amino acid residues. The regions that were taken from the crystal structure include the two transmembrane segments and the N- and C-terminal helices. The N-terminal helix encompasses residues 1-13. The TM1 and TM1 helices correspond to residues 16-41 and 73-106. The C-terminal helix comprises residues 115-131. Overall structure is similar to mtbMscL channel. The structure of in-ecoMscL is indeed similar to that of cl-ecoMscL.

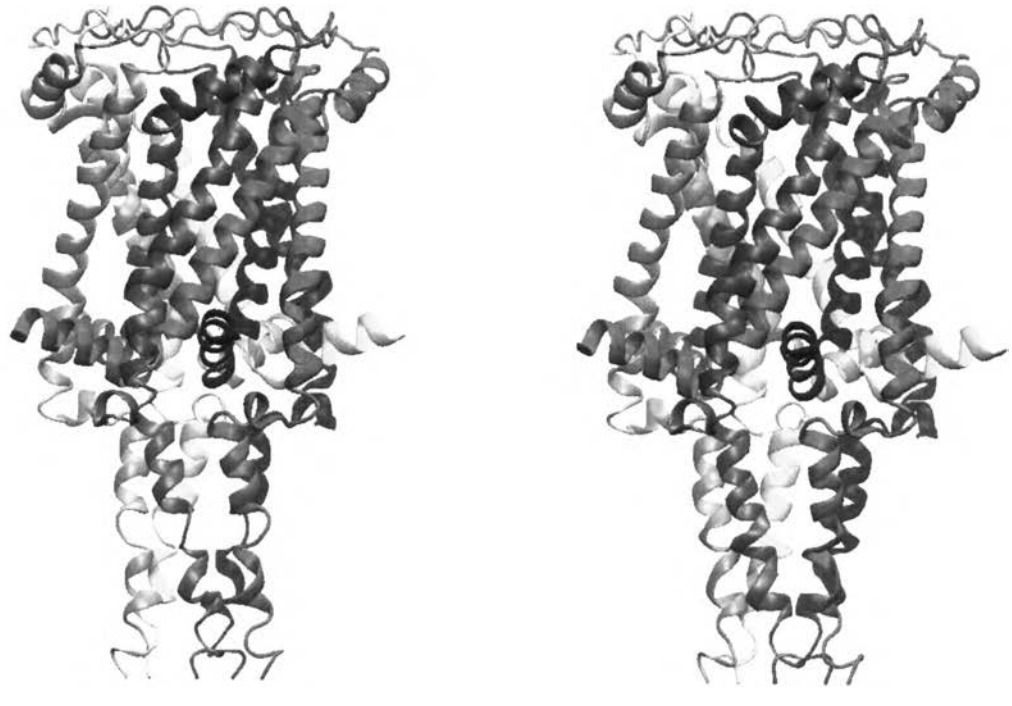

FIGURE 4.2 The conformations of EcoMscL channel in Close state (Right) and Intermediate state (Left).

The stereochemical quality of the obtained structural models of cl-ecoMscL and in-ecoMscL channel was assessed on the basis of Ramachandran diagram and G-factors of the phi (ϕ) and psi (φ) backbone dihedral angles. The distribution of the Ramachandran plot of non-Glycine, non-Proline residues are summarized in Figure 4.3. For the cl-ecoMscL model, analysis of Ramachandran plot in PROCHECK revealed that only 2% residues were in the disallowed region, while about 80% and 18% residues were found to be in the favored and allowed regions, respectively. In case of Ramachandran analysis of in-ecoMscL model, about 99.0% of the amino acid residues of these were located in the most favored and additional allowed regions.

The G-factors for dihedral angles was -0.62 for cl-ecoMscL and -0.61 for in-ecoMscL which is in acceptable range according to the acceptable G-factor in PROCHECK (-1.0), indicating a good quality of the model.

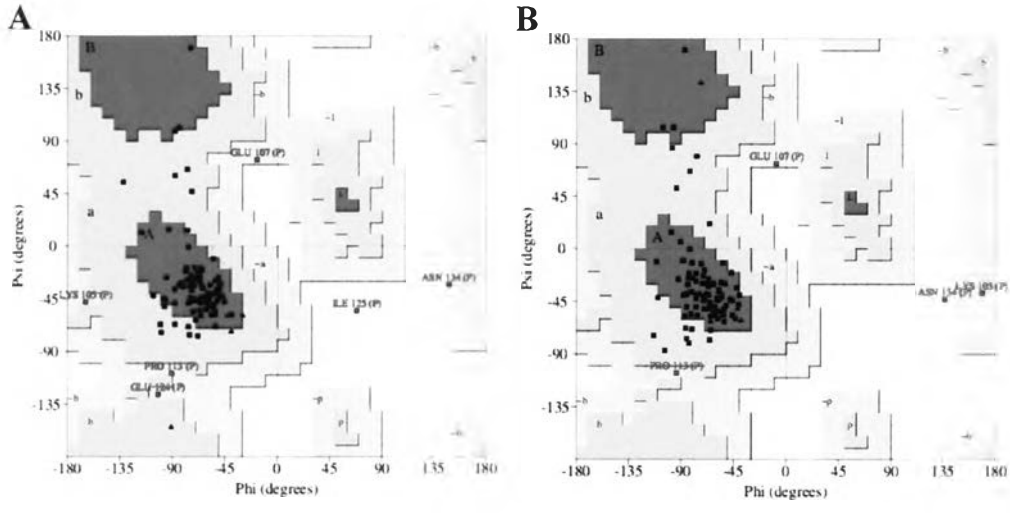

FIGURE 4.3 Ramachandran plot calculation of the psi/phi angle distribution of the model (A) Close conformation (B) Intermediate conformation, as computed by PROCHECK program.The cl-ecoMscL and in-ecoMscL structures superimpose with an overall root mean square deviation (RMSD) of about 1.8Å using all backbone atoms, and thus reveal small conformational changes between the two states. Figure 4.4 shows superimposed structural models derived from PaDSAR. As can be seen from the figure, the TM1 region exhibits the most structural deviation with RMSD of 1.8Å. Superposition of the two transmembrane domains of the in-ecoMscL onto the corresponding domains of cl-ecoMscL revealed that the cytoplasmic side of the TM1 helix is slightly tilted, resulting in a small increase of the pore diameter.

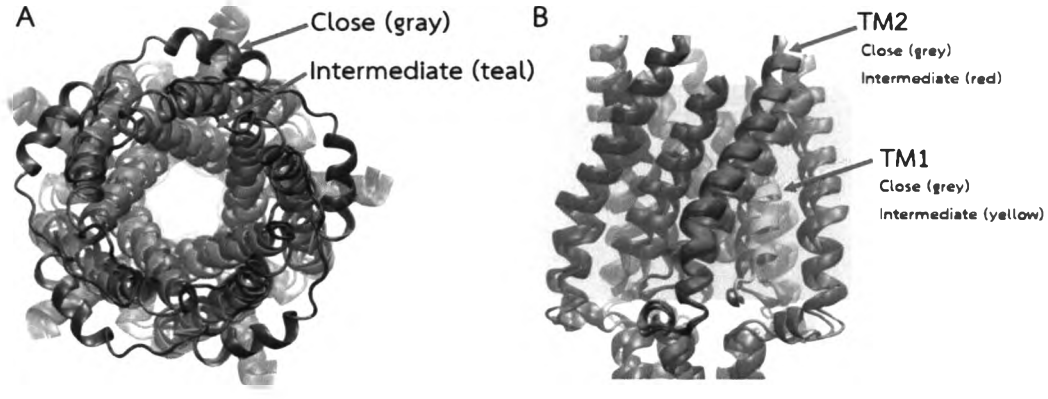

FIGURE 4.4 Represent TM1 and TM2 helices of Eco-MscL derived from PaDSAR.

(A) top view of model and (B) side view of model. The both view show the helices tilts slightly.

Inspecting the difference in the diameter of the pore between the cl-ecoMscL and in-ecoMscL conformations provides useful insight into the change in the pore radius along the ion pathway (Figure 4.4). In cl-ecoMscL, the pore is formed by a tight packing of TM1 of five subunits. The pore diameter profiles shown in Figure 4.5 illustrates that the narrowest part of the transmembrane region of the cl-ecoMscL channel has a radius of about 8 Å, and expand to ~10Å radius in the in-ecoMscL. These small changes in the width of pore diameter at the constriction point of in-ecoMscL may be associated with pre-expanded closed conformation which represents the transition pathway to the open state.

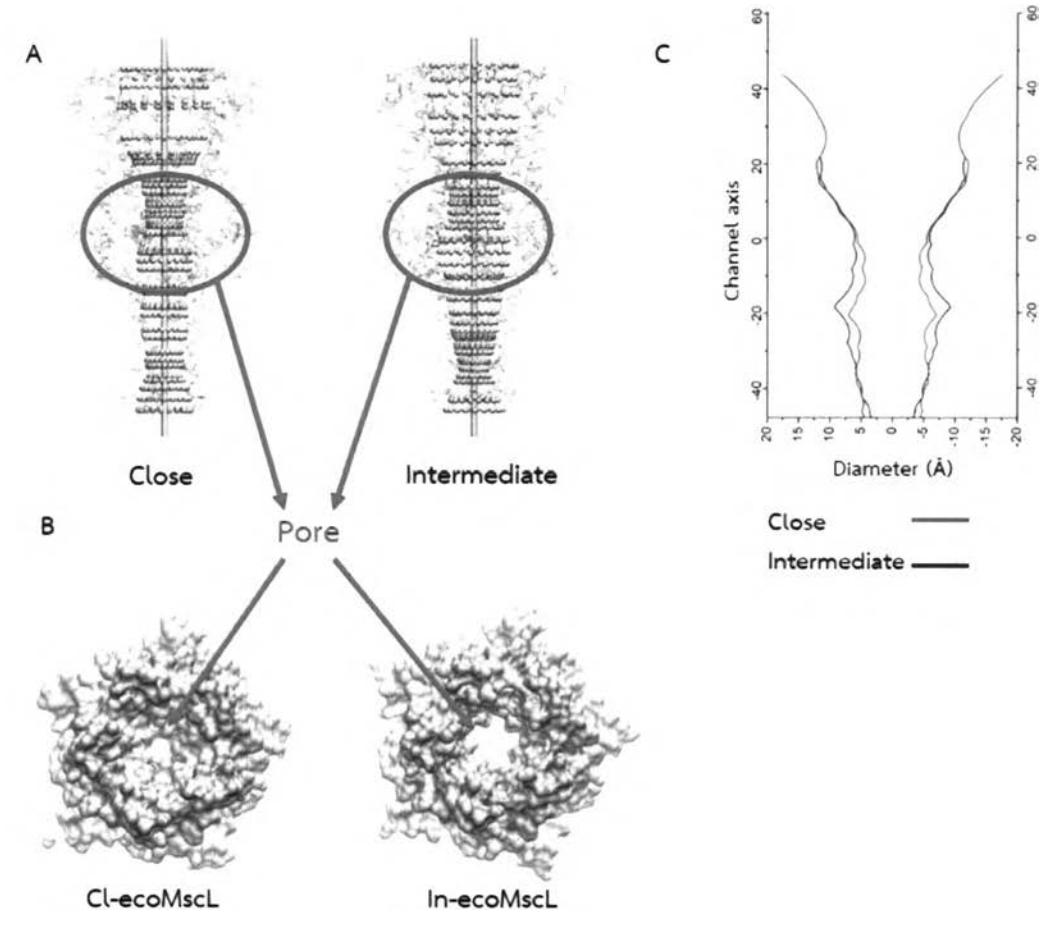

FIGURE 4.5 (A) Represented model of channel in close conformation and intermediate conformation (B) Represented by molecular surface of Eco-MscL on Top view. (C) Graphical presentation of pore diameter profiles of the closed (red line) and the intermediate conformation (blue line).

Five TM1 helices of ecoMscL are assembled together to form the inner pore, of which Leu19 and Val23 at the contriction region have been proposed to act as the main hydrophobic gate.[40] In cl-ecoMscL model, these pore-lining residues oriented its sidechains to form two hydrophobic rings. In PaDSAR model of in-ecoMscL, the sidechains of these residues at the hydrophobic gate do not significantly change its orientation. As the size of the hydrophobic gate becomes slightly larger, they loosely pack together. This can be illustrated by the number of closed contact residues plotted against residues in TM1 and TM2 (Figure 4.6). It should be noted that the compared pattern between cl-ecoMscL and in-ecoMscL shown in this plot is also in good agreement with the compared profiles of the experimental ΠO_2 between PC18 and PC12 (Figure 4.7).

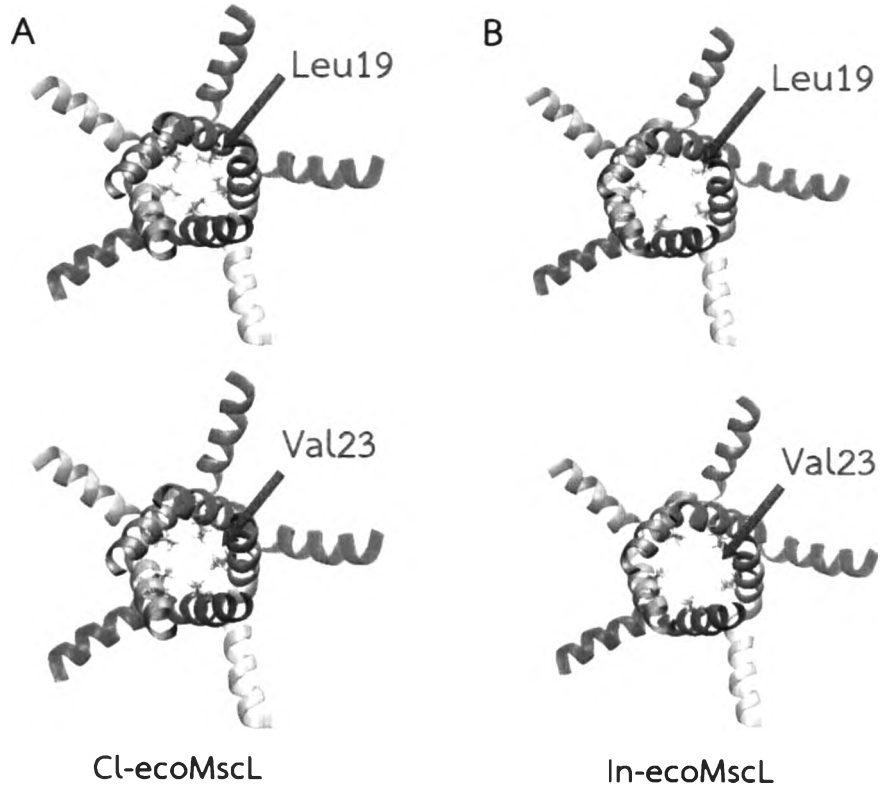

FIGURE 4.6 Movement of hydrophobic residues possibly involves with gating of *Eco*-MscL channel.

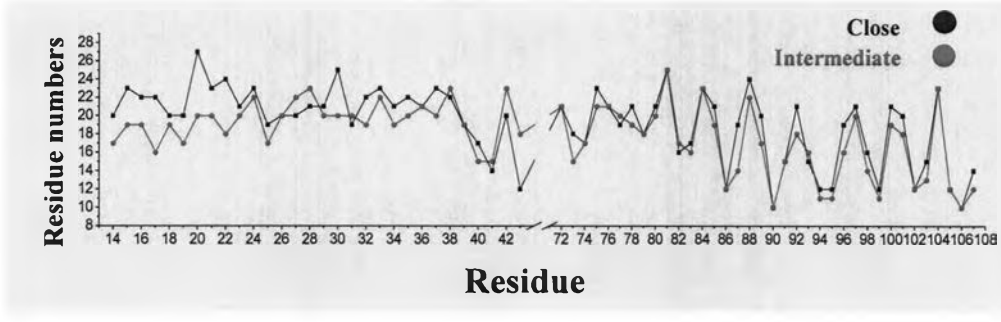

FIGURE 4.7 Number of closed contact residues along the TM1 and TM2 residues of cl-ecoMscL (black line) and in-ecoMscL (red line) models.

4.3 Structural stabilities of the cl-ecoMscL and in-ecoMscL models

The RMSD profiles of the closed and intermediate system versus the simulation time for a total of 100 ns are shown in Figure 4.8. Small RMSD values of the protein backbone atoms of cl-ecoMscL and in-ecoMscL was a result of restrained MD simulation during the first 2-4 ns. Then the RMSD value increases sharply and reach to small fluctuation with an average RMSD of 5 Å for cl-ecoMscL and 5.5 – 6.5 Å for in-ecoMscL. Besides the RMSD analysis, plots of other observable properties including the total, kinetic and potential energy parameters, temperature, pressure and volume suggested both MD systems are thermodynamically equilibrated and well behaved. Thus the MD trajectories were used for further structural analyses.

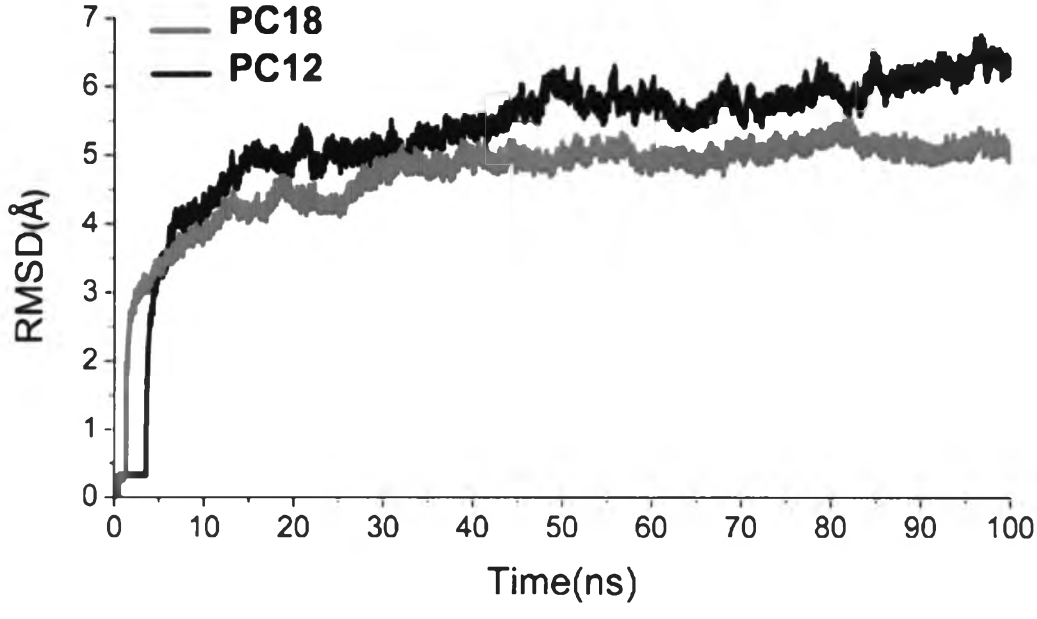

FIGURE 4.8 Backbone RMSD with respect to the starting structure of two MD systems as a function of simulation time.

Figure 4.9, shows the RMSD as a function of simulation time for different domains (TM1, TM2, extracellular loop, N- and C-terminal) of cl-ecoMscL and in-ecoMscL models. For cl-ecoMscL, the RMSDs of the two transmembrane and N-terminal helices are smaller than those of the C-terminal domain and extracellular loop. The RMSD curves of the two transmembrane helices increase and reach a small fluctuation around 2-3 Å with respect to the starting structure, suggesting structural stability of transmembrane portion of the channel. Similarly, structural stability of the transmembrane region of the channel was observed in the in-ecoMscL model with an average RMSD fluctuation of 2-3 Å. This also suggested a well packing of the inner transmembrane segments. It was also found that, the RMSD of extracellular loop of both simulated systems is relatively larger than those of the remaining domains. These results suggest that the extracellular loop of ecoMscL is highly flexible in both closed and intermediate conformations.

The structural stability for individual chain is illustrated in Figure 4.10. For cl-ecoMscL, all five chains exhibits similarRMSD profiles within a range of 3 to 5 Å fluctuation. The results indicates that ecoMscL forms a stable transmembrane assembly as pentamer in it closed conformation. For the intermediate state models, distinct structure deviation is observed from RMSD values between Chain B and Chain E helices after 40 ns. The results implies asymmetric motion of ecoMscL channel in the intermediate conformation.

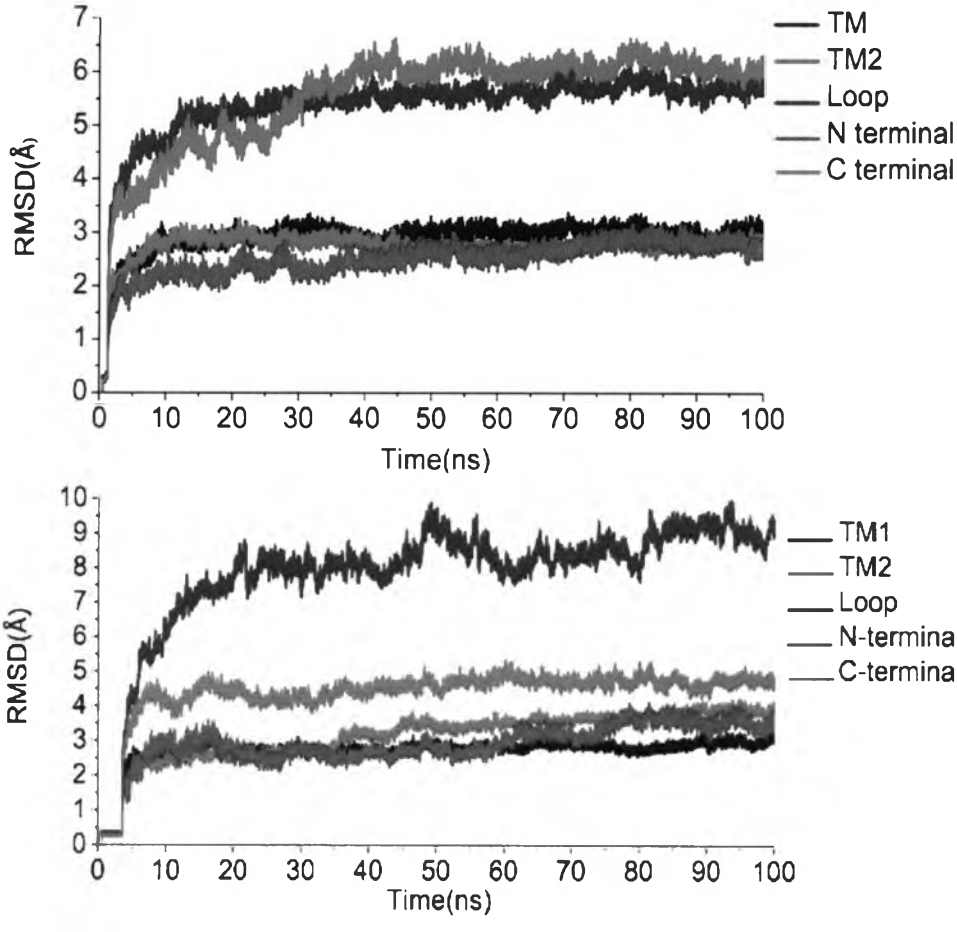

FIGURE 4.9 The RMSD profiles of the different domain (TM1, TM2, Periplasmic loop, C terminal and N terminal) of two MD system as a function of time.

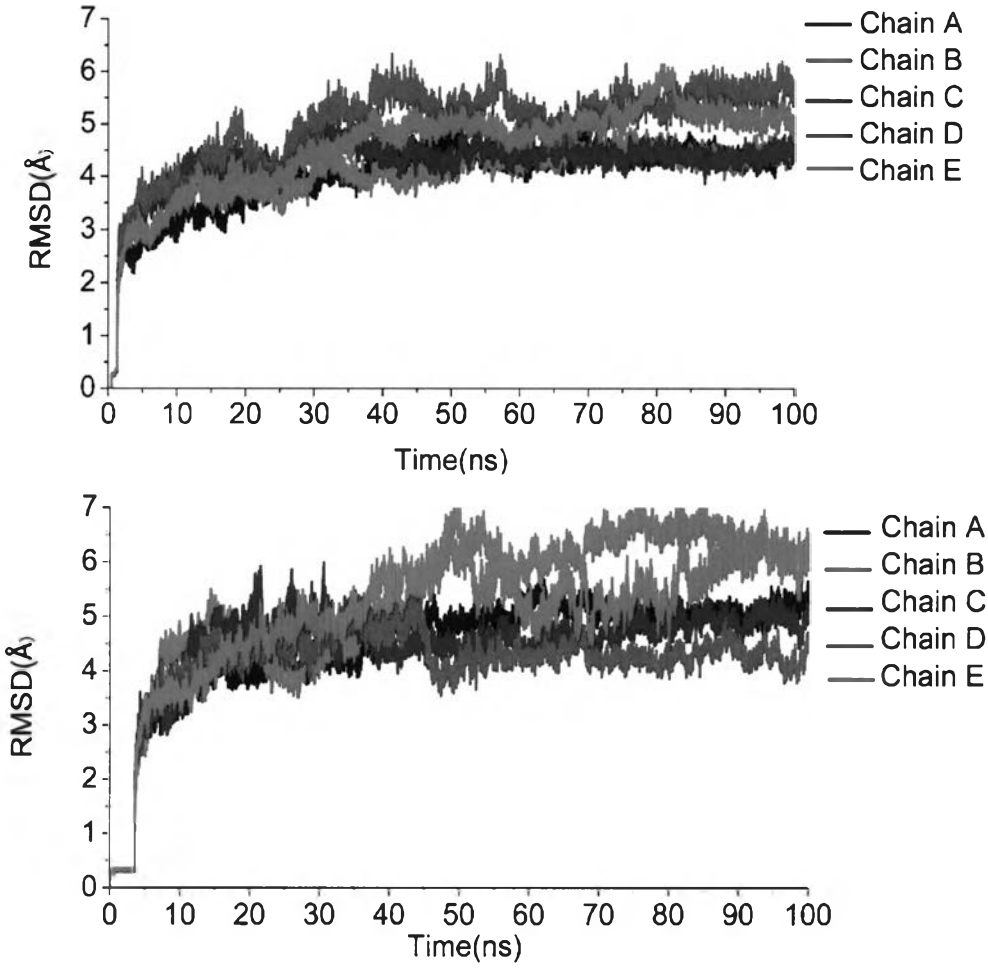

FIGURE 4.10 RMSD of individual TM segment (Chain A-E) of two MD systems (Up is a close conformation and Down is a intermediate conformation) as a function of time.

Monitoring protein dynamics from the simulations have been achieved by computing root mean square fluctuations (RMSF). An analysis of structure fluctuation with respect to the average structure. Figure 4.11, shows the average RMSF per-residue of cl-ecoMscL and in-ecoMscL models measured during the last 10 ns of the trajectories. Comparison of the RMSF values of cl-ecoMscL and in-ecoMscL for TM1 (residue 14 to 43) and TM2 (residue 72 to 107) revealed no significant difference in protein dynamics between the closed and intermediate conformations. The greatest changes in structural dynamics were detected at the extracellular loop. The loop of in-ecoMscL exhibits larger backbone flexibility than that of the cl-ecoMscL. As described previously, the nature of hydrophobic interactions between methylene groups from large numbers of fatty acyl chains and shallow grooves at the transmembrane surface of MscL provides a tight packing of transmembrane α-helices within the lipid bilayer. One can see that the flexibility of the extracellular loop in intermediate conformation is larger than that of the extracellular loop of close conformation due to influence from the membrane thickness shorter than the close conformation. Thus the interaction of acyl group of DLPC within transmembrane α-helices is somewhat weaker than that of POPC.

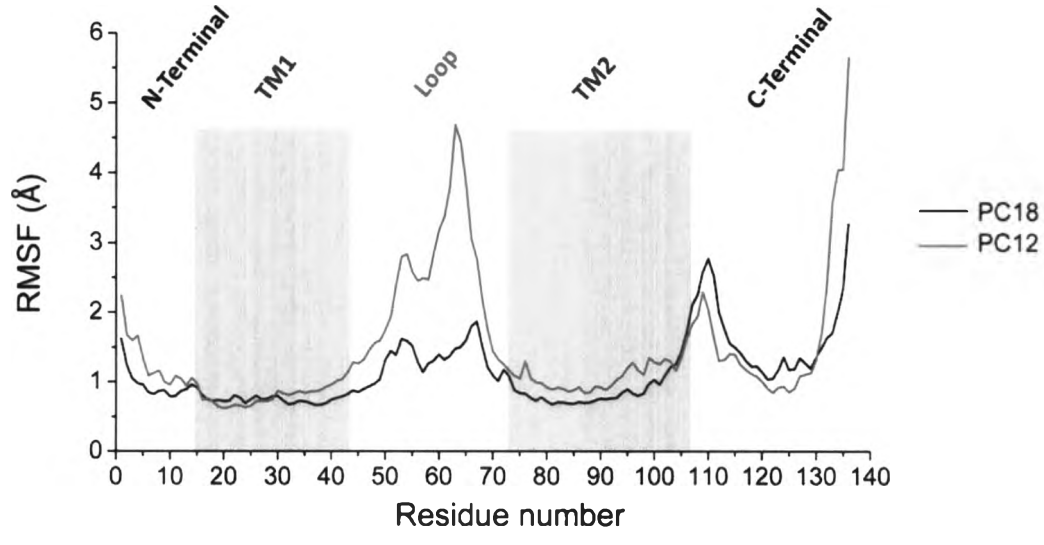

FIGURE 4.11 Average backbone RMSF of closed system (I) (black) and Intermediate system (red). Illustrate the different domains (TM1, TM2, Periplasmic loop, C terminal and N terminal) of proteins.

Furthermore, RMSF of backbone atoms of cl-ecoMscL and in-ecoMscL for each subunit were calculated to elucidate the flexibility of individual chain of the protein (Figure 4.12 and Figure 4.13). The results show that RMSFs of each subunit share an overall similar pattern of structural dynamics. The extracellular loops have large RMSF while the two transmembrane domains have low RMSF.

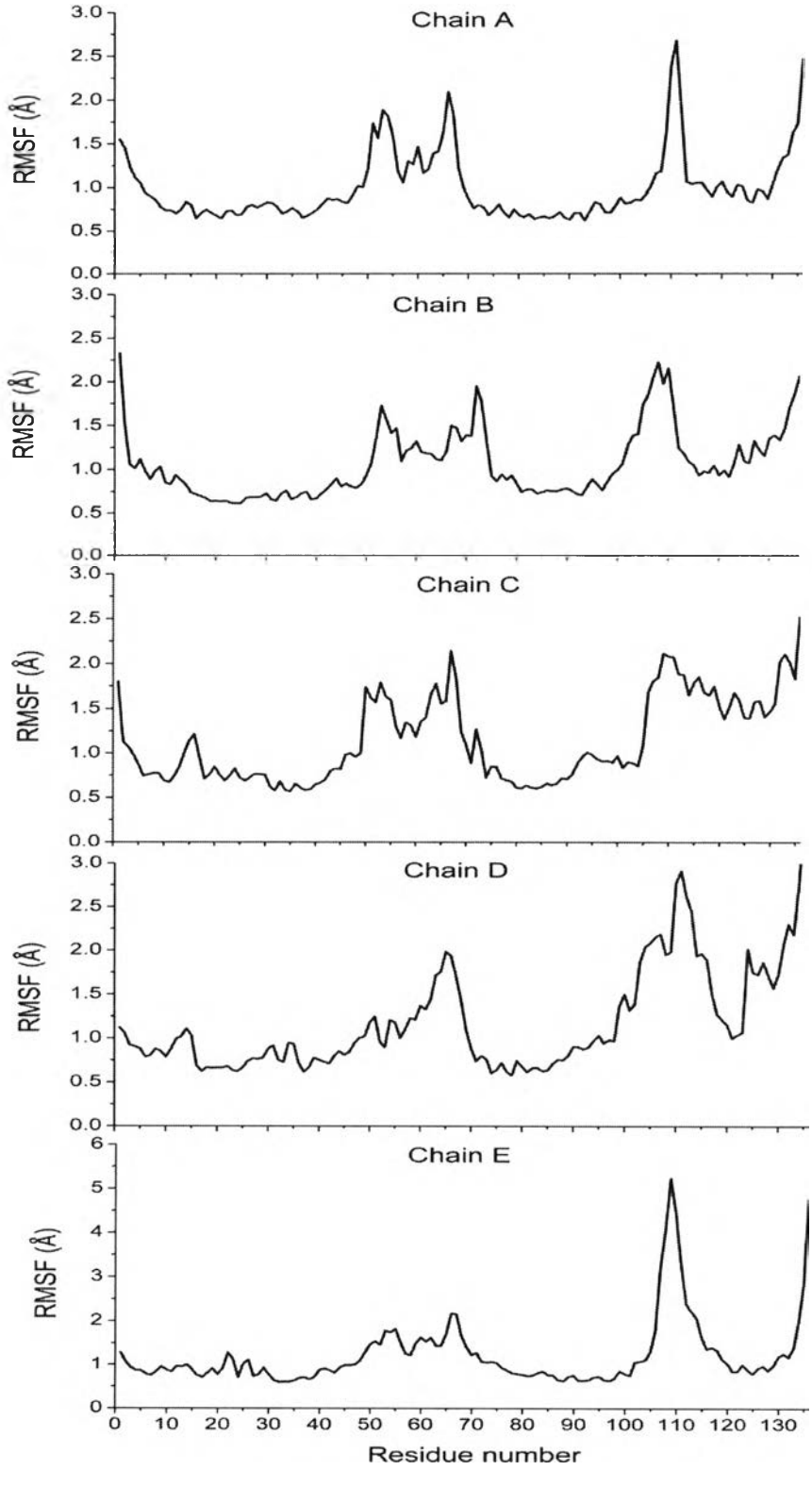

FIGURE 4.12 Backbone RMSF as a function of residue number of close state (PC18).

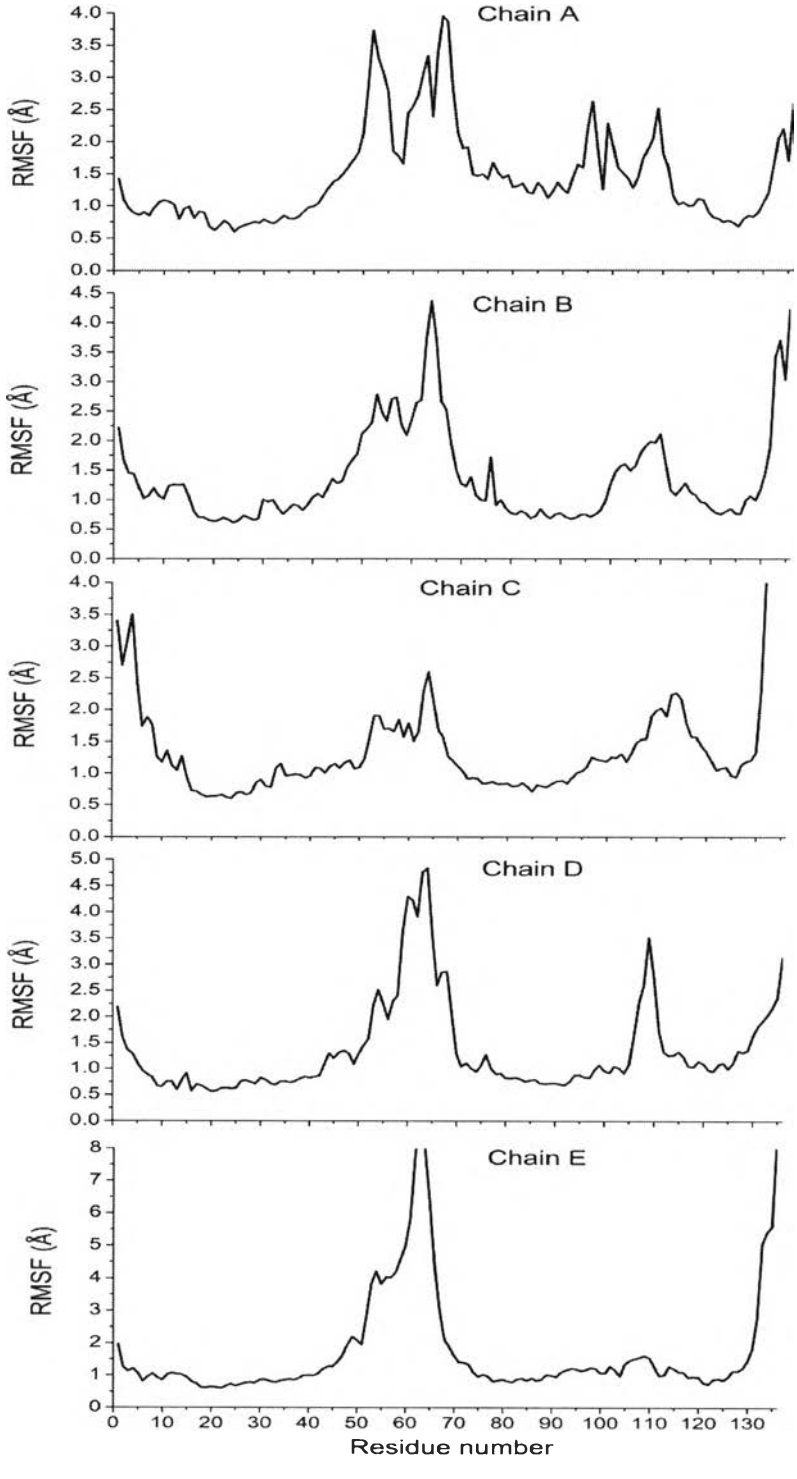

FIGURE 4.13 Backbone RMSF as a function of residue number of intermediate state (PC12).

The structural flexibility of the two transmembrane segments obtained from RMSF analyses have been validated by comparing with experimental data. The RMSF for TM1 and TM2 are represented by statistical box and whisker diagram as shown in Figure 4.14. A comparison between the RMSF data of cl-ecoMscL and in-ecoMscL systems and the experimental mobility parameter (ΔH_0^{-1}) obtained from SDLS/EPR technique revealed a great consistency. The overall trend of both data shows that the TM2, which is an outer transmembrane segment is slightly more dynamics than the inner TM1 segment (left). This result is in good agreement with the mobility data (up).

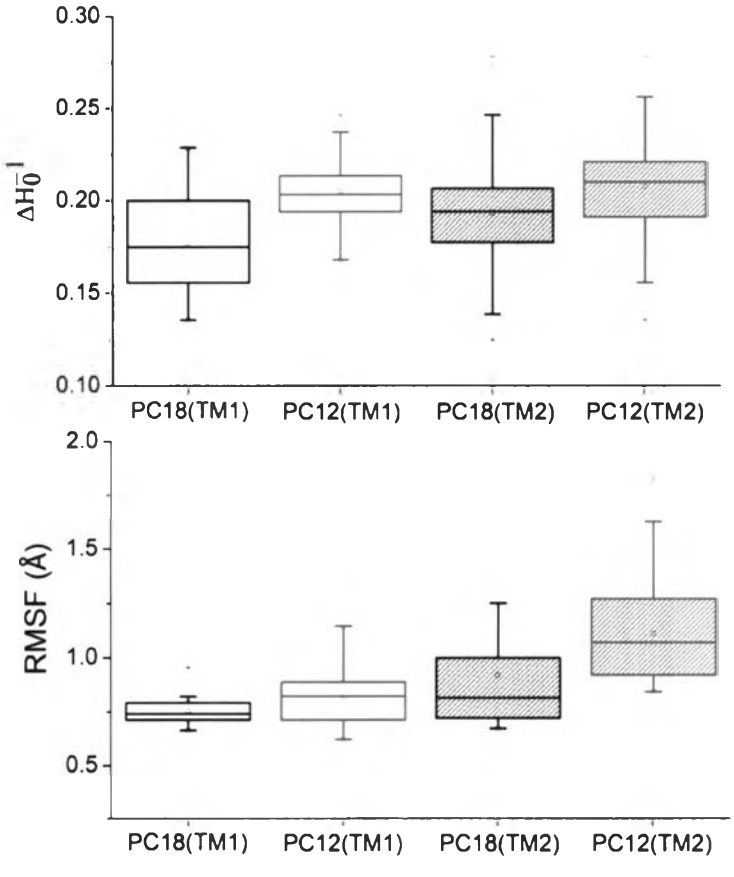

FIGURE 4.14 RMSF box plot of accessibility data from EPR (Up) and alpha carbon of two transmembrane helices (Down). The bottom and the top of the box are 25 and 75 percentile. The median is the straight line, and the mean is plotted as a square.

To verify the stability of secondary structure of transmembrane helices, an analysis of the secondary structure of protein as a function of time was illustrated in Figure 4.15. Overall profiles of secondary structure pattern show a major stability of α-helical conformations of each segment. TM1 and TM2 (the red color region) of cl-ecoMscL systems remains significantly unchanged during the course of the simulation. This indicates that the transmembrane helices were stable over the simulation time. One can see such as a continuous red color and smooth band of the TM1 and TM2 helices. The secondary structure profile of in-ecoMscL system (Figure 4.15) shows the same stability pattern of helical conformation similar to that of cl-ecoMscL. All results together suggest that ecoMscL undergoes rigid body motion between the closed and intermediate states.

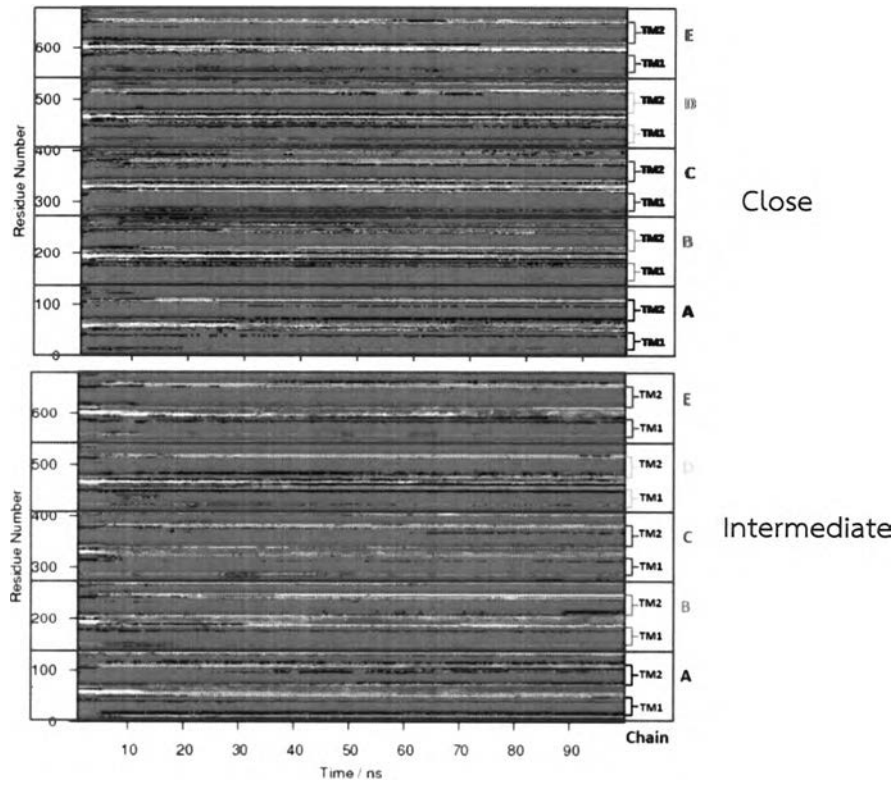

FIGURE 4.15 Show that stability of secondary structure helices of the five transmembrane segments included TM1 and TM2 of close state and intermediate state as a function of simulation time calculated by DSSP. The each color mean : α-helix (red), stand in β-sheet (blue), β-bridge (yellow), β-turn (black), coil (green), unassigned (white).

4.3 Inter-subunit distance changes at the hydrophobic gate residues

It is more intuitive to measure inter-subunit distances to indicate such small conformational changes. Structure models derived from PaDSAR and ΠO_2 data illustrate the most significant changes occurred near the hydrophobic gate. The hydrophobic constrictions of the inner pore of the channel involve the two hydrophobic residues: Val-23 and Leu-19. As a homopentameric protein with five-fold symmetry, the inter-subunit distances of these residues which are defined as "short" and "long" distance were measured from the simulation. The "short" distance defined an intersubunit C_α–C_α separation of the residue between a subunit and its first adjacent subunit whilst the "long" distance defined that of the residue between a subunit and its second adjacent subunit. Figure 4.16, shows the short and long inter-subunit distances. It appears that both short and long intersubunit distances of in-ecoMscL is greater than those of cl-ecoMscL.

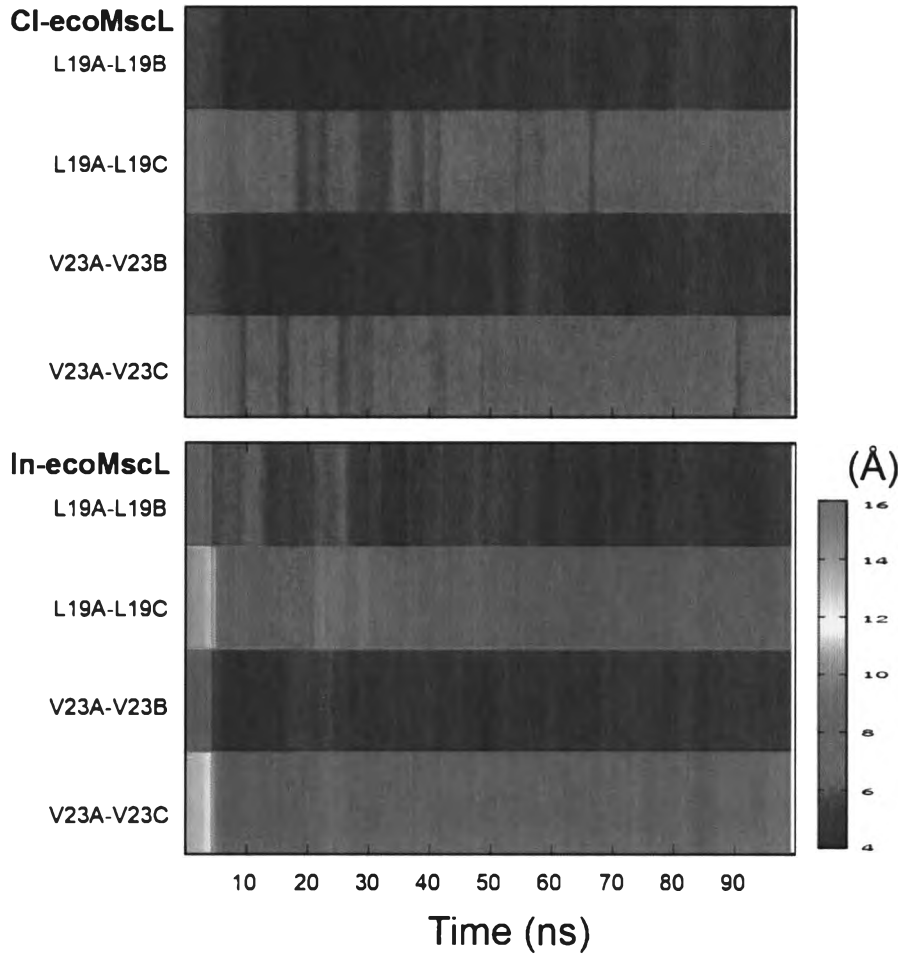

FIGURE 4.16 Color scale represents the distance pair of gated of channel in Eco-MscL in close state and intermediate state.

4.4 Protein-induced lipid perturbation

The matching between the hydrophobic thickness of the lipid bilayer and the hydrophobic surface exposure of the protein has been found to play important role of structure stability, protein regulation and function. In an effort to elucidate the effects caused at the molecular level by the lipid-protein hydrophobic mismatch, MD simulations of cl-ecoMscL and in-ecoMscL were performed using a different length of the lipid chain. The MD simulation of cl-ecoMscL was carried out in 18-carbon of POPC lipid while the in-ecoMscL simulation was done in 12-carbon DLPC (Figure 4.17). Apparently, the hydrophobic thickness of the bilayer model of pure POPC is about 4 Å greater than that of pure DLPC bilayer. Figure 4.17, shows the membrane thickness profiles of the simulations in the presence of cl-ecoMscL and in-ecoMscL. During the first 5ns of simulation, the width of POPC bilayer appears to compress from 40Å to as low as 33Å whereas that of DLPC bilayer tends to expand from 28Å to 30Å. The average membrane thickness for the last 20ns of simulation was 34.6Å for POPC bilayer and 31.9Å for DLPC bilayer. This observation is supported by measuring the bilayer thickness that is 39.1Å for POPC and 32.6Å for DLPC.[41] At this point, the in-ecoMscL simulation gave the results of a bilayer thickness closer to the experimental observed value whereas the results of the cl-ecoMscL simulation exhibits a shorter thickness of POPC bilayer. Thus the effect of the protein-induced bilayer perturbation was greater in the cl-ecoMscL.

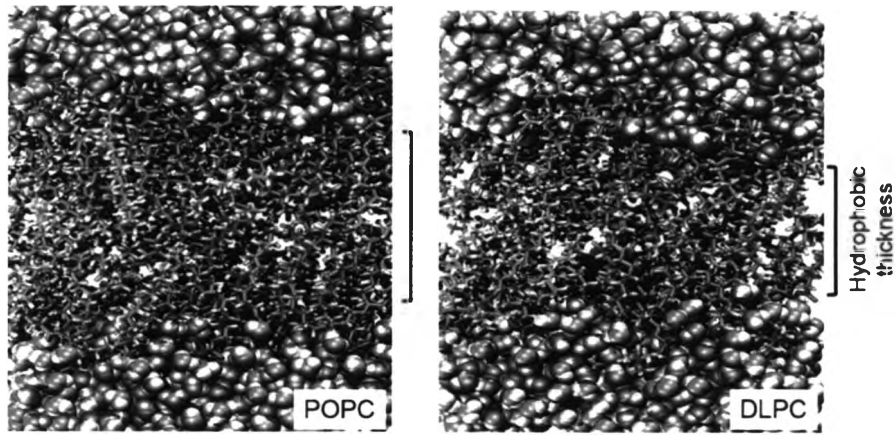

FIGURE 4.17 Hydrophobic thickness of pure POPC bilayer is about 4 Å greater than that of DLPC bilayer.

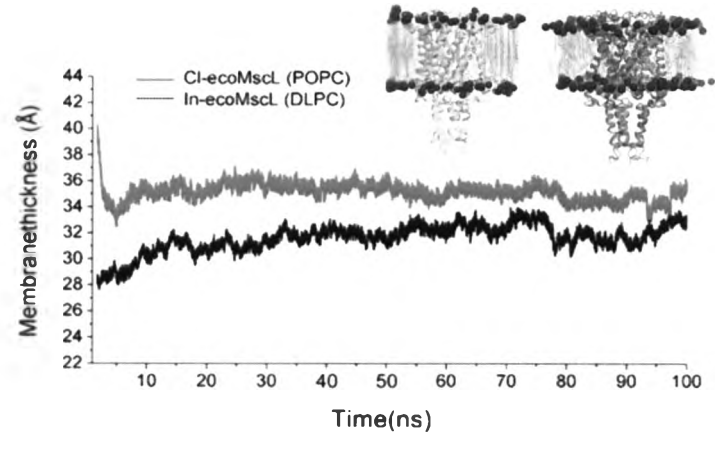

FIGURE 4.18 Membrane thickness profiles of POPC and DLPC bilayer obtained from the simulations in the presence of cl-ecoMscL and in-ecoMscL, respectively. The thickness was measured from an average distance between the N-atom of tertiary amine head group.

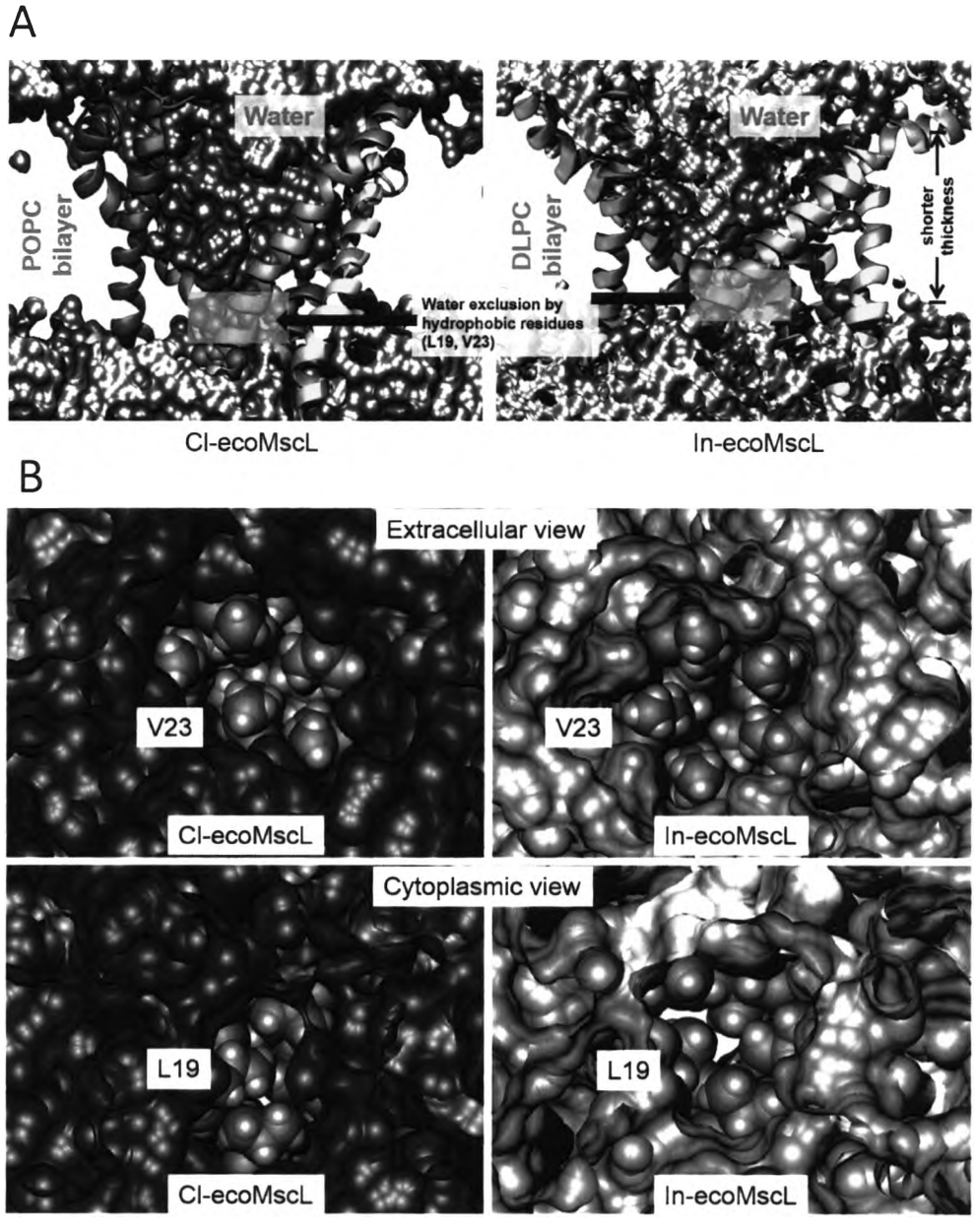

FIGURE 4.19 The closed gate in the pore at the constriction region occluding the passage of water. (A) Water molecules enter to the pore but do not penetrate throughout the channel. Water occlusion is located near the narrowest region of the pore (orange) constituting of two hydrophobic residues, L19 and V23. (B) Extracellular and cytoplasmic views illustrate these residues forms a hydrophobic plug.

4.5 Proposed transition model.

Structure models derived from PaDSAR and an analysis of the MD results revealed small changes between closed to intermediate conformations. The key conformational change is associated with the motion of both transmembrane helices and N- and C-terminal domains. The structural rearrangement results in a loose packing between TM1 and TM2. The results observed from the MD simulations are consistent with the experimental mobility, suggesting the TM1 is more conformationally mobile than the TM2 with has been previously.[42] However, an overall structural movement does not significantly enlarge the pore radius at the constriction region. Side chains of the two gating residues Val23 and Leu19 prevent the passage of water. Interestingly, the in-ecoMscL conformation obtained from this study might correspond to a non-conducting intermediate state. An existence of this conformational state has been supported by the recent crystallographic structure of tetrameric MscL from Staphylococcus aureus (saMscL). The saMscL structure is not in closed state but still non-conductive. It has been proposed that it corresponds to a pre-expanded closed conformation.[43]

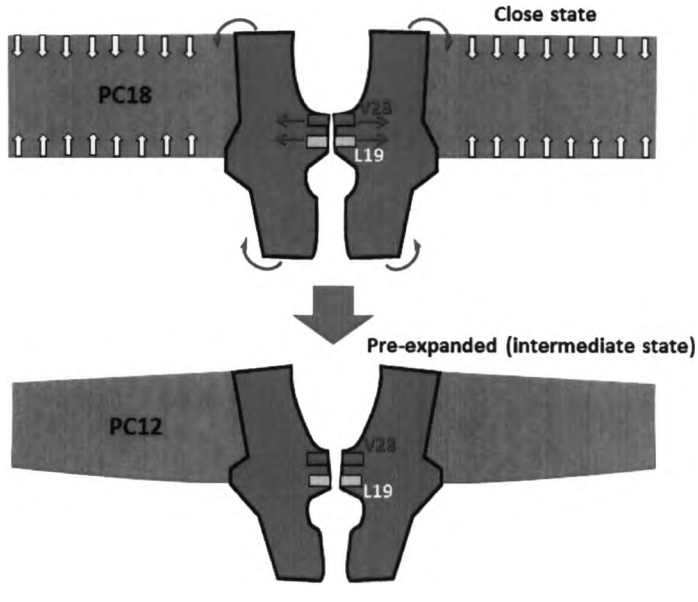

FIGURE 4.20 Proposed mechanism for the closed - intermediate transition.